CHAPTER IV

SATELLITE IMAGE AND AERIAL PHOTOGRAPHIC INTERPRETATION

In this chapter, description is divided into three sections. The first section is focussed on geological lineament interpretation in a regional scale. The area of interest covers the Phrae and Lampang basins of northern Thailand. Both Landsat TM5 and JERS SAR imageries are applied tools for this interpretation. The second section describes on fault segmentation of the Phrae fault system, and focus is placed upon the southeastern segment of this fault system. In addition, tectonic geomorphology interpretation using aerial photograph is emphasized in the last section. Tectonic geomorphological map, which includes fault branch and geomorphic evidence of fault movement, is also shown in this section.

4.1 Lineaments

Lineaments are referred to a linear feature found in the earth's surface. This feature can be delineated on map or on aerial or satellite images, which be at least a few kilometers long (O' Leary et al., 1976). Various lines of disruption, which separate areas of different weathering and erosion, morphologic and geologic feature, are also referred to lineaments (O' Leary & Simpson, 1977). Normally, lineaments have been found influence with straight or curvilinear streams and valleys, topographic alignment, boundary between area and morphology or slope, and linear trend due to both lithologic change or break. These surface breaklines are often observed related to tectonic activity (Strandberg, 1967). Moreover, lineaments have also referred to significant lines of landscape which reveal the hidden architecture of the rock basement (Hobbs, 1972). In addition, real lineaments are surface expression of faults or fault zones, together with associated structures (Park et al., 1994). Satellite remote sensing imagery, which provides raw data in both regional and local scales, plays an important role in lineament analysis of structural and geotectonic investigations related to earthquake studies. Remote sensing data is a useful tool to understand geological framework of the region due to inexpensive, time-effective, and relatively accurate information (Charusiri et al., 1996).

In an attempt to understand regional characteristic and pattern of geological lineaments in the study area and nearby, Landsat TM5 and JERS SAR imageries were conducted for lineament interpretation approach. Landsat

TM5 image (taken on 10/Feb/1991) is a false-coloured composites (band 4, 5, and 7 in red, green, and blue, respectively) at scale 1:250,000 covering Lampang and Phrae basins and some part of Nan and Sukhothai basins (Figure 4.1). In addition, JERS SAR image at scale 1: 500,000 covering the Phrae basin and nearby areas were applied for analysis as well (Figure 4.2). Identification of lineaments was performed by visual justification. Traceable lines are layout on hard copy prior to digitally modified using Map Info program. Additionally, rose diagram was also conducted to indicate frequency of lineaments in eight directions (N, E, NE, NW, NNE, NNW, ENE, and WNW) and their lengths.

4.1.1 The Result from Landsat TM5 Interpretation

Lineament interpretation using Landsat TM5 is shown in Figure 4.3. The major trends of lineaments lie in NE and NNE, and the minor trends are in N, NW, NNW, E, ENE, and WNW. Lineaments with long distance are found aligned in the NE trend, besides, the shorter are observed in almost all direction.

The longest lineament, which is referred to Thoen fault (Fenton, et al., 1997 and Srisuwan et al., 2000) is located at the bottom left of the map. This fault with the NE trend is observed in the northern part of the Thoen basin and apparently extends to the Phrae basin. The fault shows horsetail-splay characteristic, which is normally found in strike-slip regime (Chistie-Blick & Biddle, 1985). The other interested lineament is a long lineament, found at northeastern part outside the Phrae basin near Rong Kwang district. This lineament also lies in the NE trend in the mountainous area, which seems to connect between the Phrae basin in the southwest and the Nan basin in the northeast. In addition, two long NE-trending lineaments are delineated at southeastern part of the Mae Moh basin. These lineaments are referred to be parts of Thoen fault and characterized as fault-bounded basin (Fenton et al., 1997). In the northeastern part outside the Sukhothai basin, there is long, NE-trending found lineament in mountainous area. This lineament is believed to be part of Uttaradit fault zone (Tulyatid & Charusiri, 1997).

As shown as dashed box in Figure 4.3 and based on Landsat lineament map, three fairy defined lineament sets are recognized in the study area within the Phrae basin. Two long and distinct, the northern and southern branches, lineaments can be traced in the NNE trend along the mountainous front. These two lineaments are almost

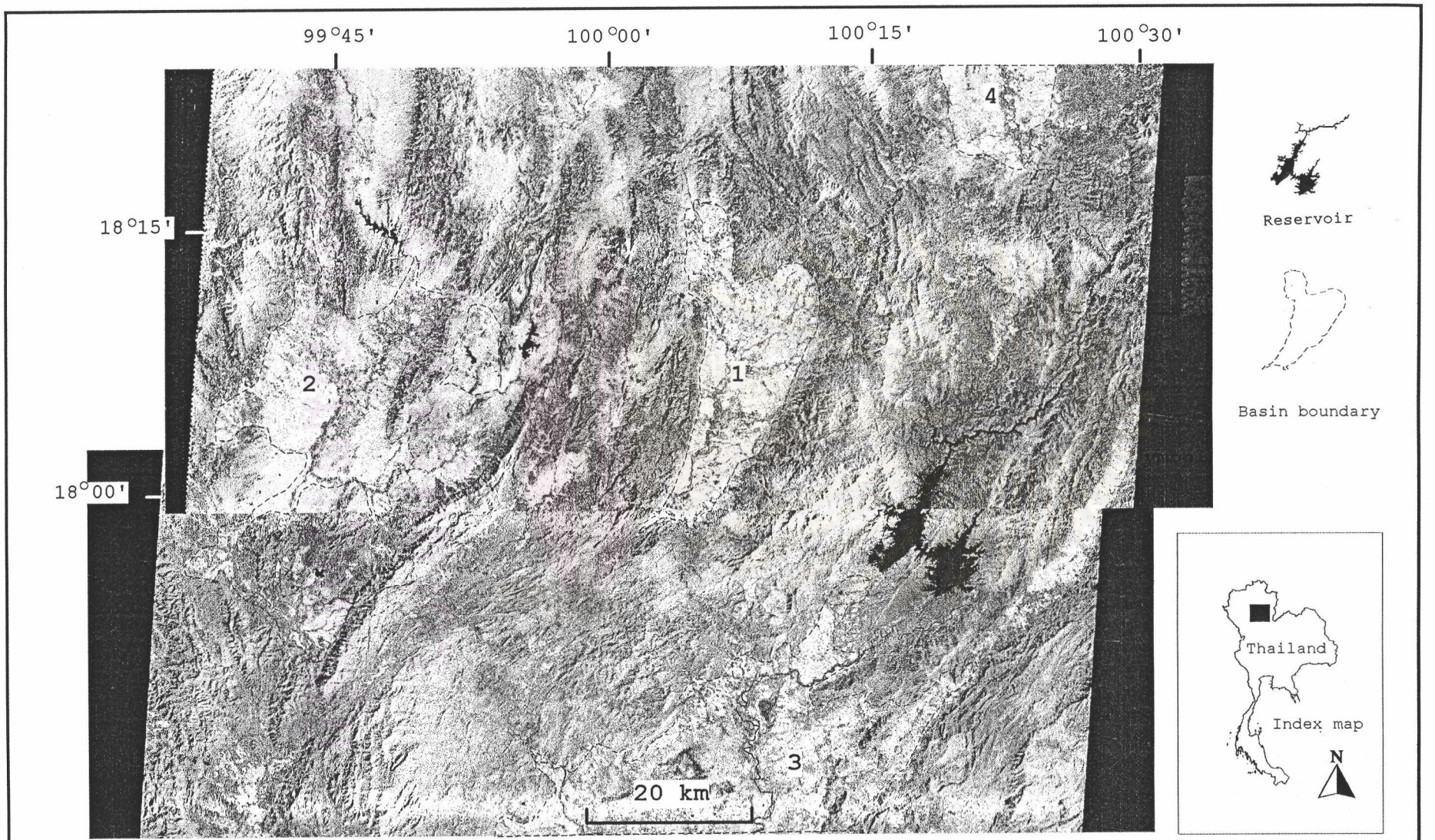

Figure 4.1 Landsat image data showing location of the Phrae basin(1) the Lampang basin(2), the Pitsanulok basin(3), and the Nan basin (4).

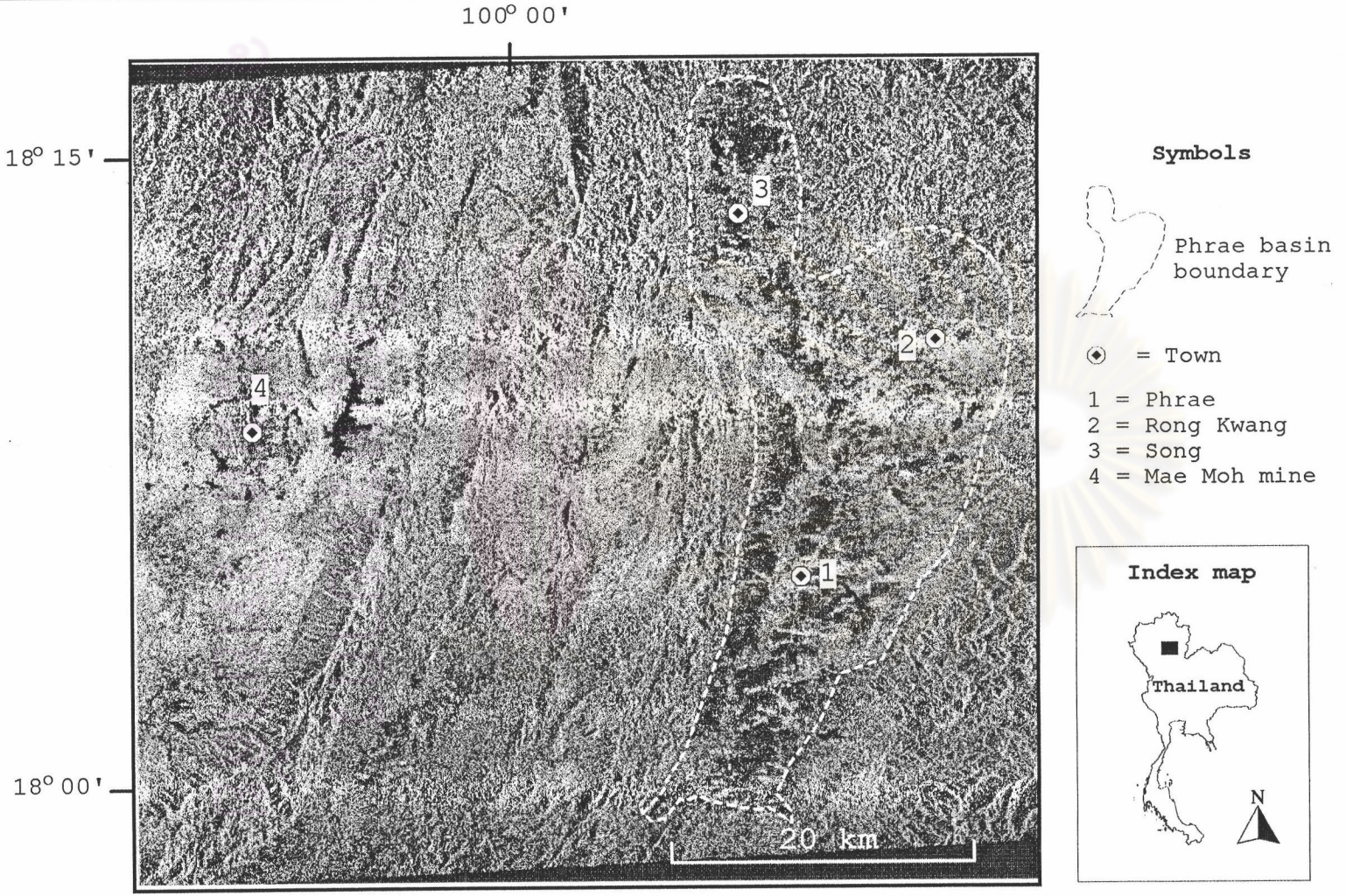

Figure 4.2 JERS SAR image data of the Phrae basin and nearby areas.

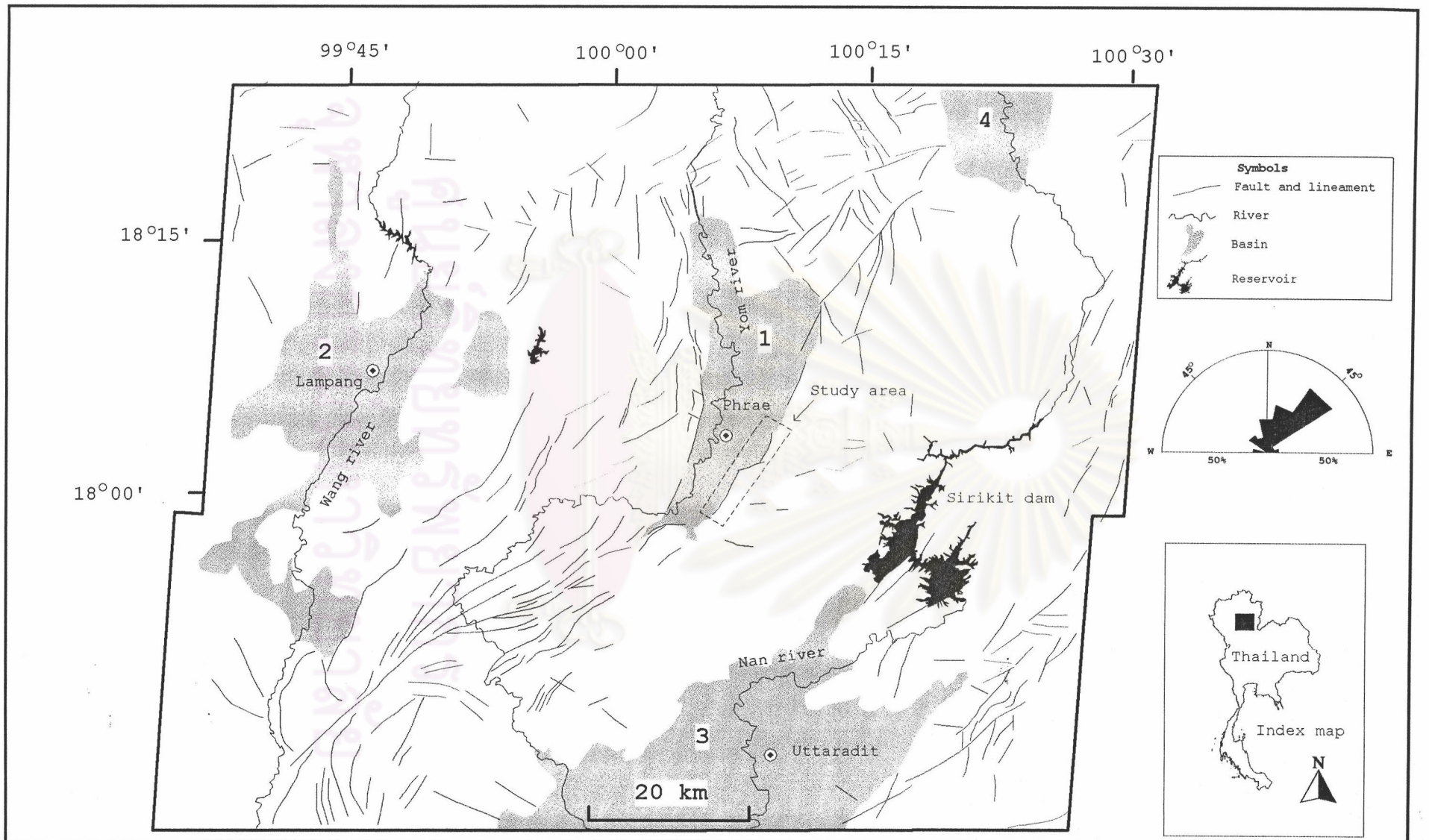

Figure 4.3 Lineament map of the Phrae basin and adjacent areas interpreted using Landsat TM5. 1=the Phrae basin; 2=the Lampang basin; 3= the Pitsanulok basin; 4= the Nan basin. Rose diagram showing major lineaments lie in NE- and NNE-trend.

parallel to each other. The other lineament which is located between these two lineaments, strikes in the ENE trend and seems to pass through the Phrae basin.

Lengths of the southern and northern NE-trending branches are about 13 km and 7 km, respectively. The ENE-trending lineament is about 5-km-long.

According to structural geometry of these lineaments, the ENE-trending segment seems to displace the eastern edge of the Phrae basin. Therefore, it is apparent that the ENE-trending lineament cut across the NNE-trending lineaments into two separated lines with right lateral movement. Tectonic geomorphology from both aerial photographic interpretation and field investigation also support this appearance.

4.1.2 The Result from JERS SAR Interpretation

JERS image acquired from radar transmission method has an advantage to penetrate several depths of sedimentary basins in arid regions, either day or night times, and in condition of cloud or fog covers (Slemmons & DePolo, 1986).

In this study, the result shows that lineaments are found in the entire region covering both basins and mountainous areas. Almost all lineaments are fairly defined and shown in the map as dash line. Only four lineaments have clearly seen, which are referred to the Thoen fault shown in solid line. Mostly, lineaments are displayed with short length. Major trend is found lying in NE- and NNE-trendings and minor is in N-, NW-, NNW-, E-, ENE-, and WNW-trendings (Figure 4.4). According to the Phrae basin, there are several lineaments that have been detected both within the basin and around the basin boundary. All of these lineaments are observed clearly in the central and the lower parts of the basin.

Based on the result of JERS image interpretation, there are three major lineaments including the northern and southern NNE-trending and the central ENE-trending lineaments. The alignment and location of these lineaments resemble those interpreted using Landsat TM5. However, in JESR image, the length of the ENE-trending lineament found longer than those of the Landsat image, which is traceable further to southern part of the basin.

In conclusion, results from both remote sensing information in regional scale reveal the major trend of geological lineaments in the NE and NNE directions, and

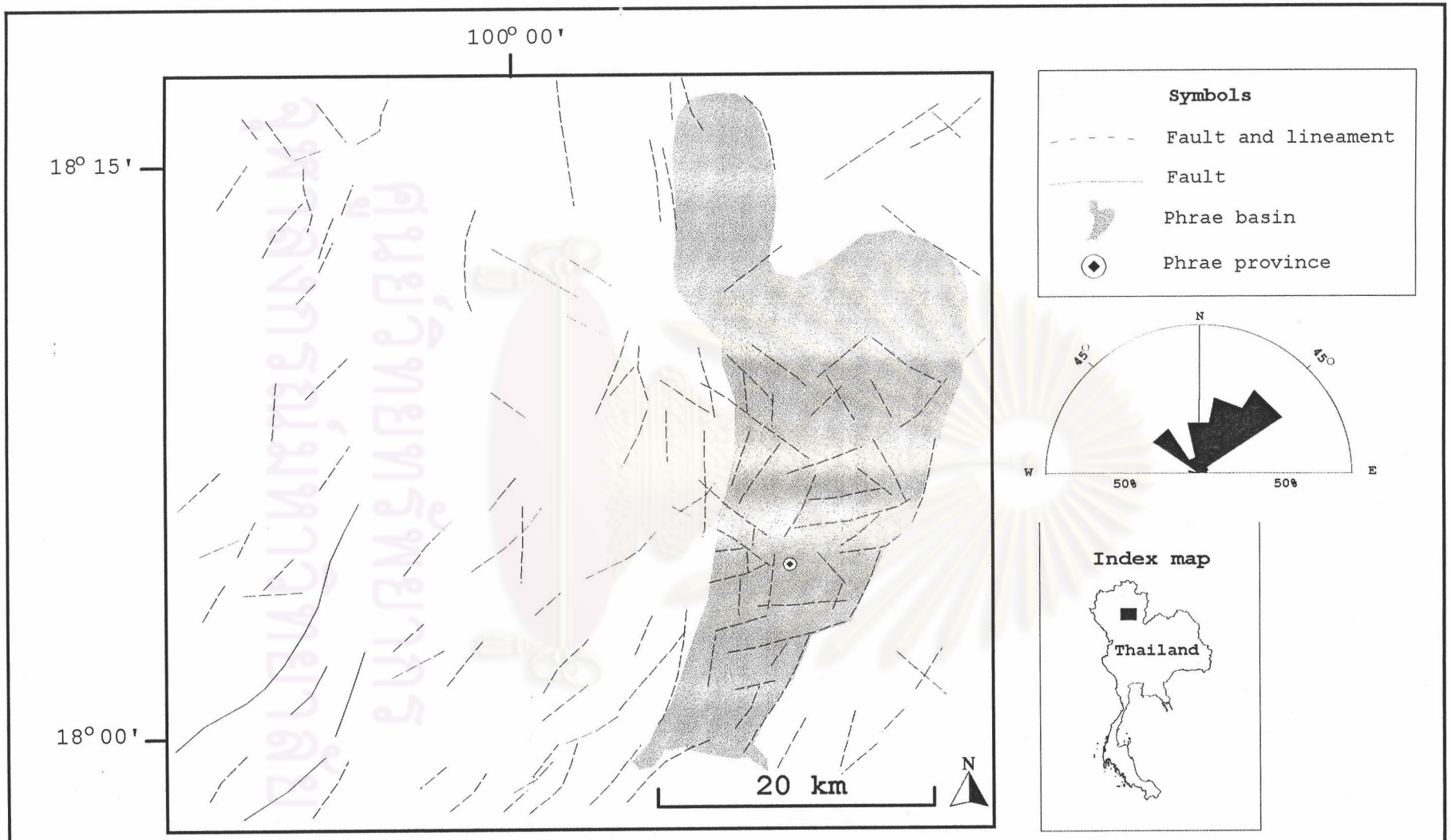

Figure 4.4 Lineament map of the Phrae basin and nearby areas interpreted using JERS SAR image data showing lineaments within the basin. Rose diagram represents major lineament trending in NE and NNE.

the minor trend in N, NW, NNW, E, ENE, and WNW directions. Most lineaments are short with the average length of about 10 km. However, the longest one is more than 70 km and located at northeastern part of the Thoen basin. In the study area, there are three major lineaments i.e., two NNE-trending lineaments with the average length of 9 km and the ENE-trending one with the length of 5 km. The latter seems to displace and separate the two formers by right lateral movement.

4.2 Fault Segmentation

4.2.1 General

Concept of fault segmentation is elucidated by the fact that historical surface rupture triggered by earthquakes along the long faults seldom occurred throughout the entire length, only one or two segments became ruptures during large earthquake (McCalpin, 1996). For instance, the San Andreas Fault zone of California was divided into four segments based on difference of historical surface rupture (Allen, 1968). The long fault trace is composed of numerous discrete segments (Segall & Pollard, 1980). The segmentation of fault systems is related to the identification of individual fault segments, based on continuity, character and orientation. It is recommended that a segment can rupture as a unit (Slemmons, 1982). Aki (1984) suggested that the delineation of segments is related with the identification of discontinuities in the fault system. Discontinuity can be divided into two main groups; geometric and inhomogeneous. Note that this statement has borrowed from seismologists who have used these terms for asperities and barrier. In addition, it is believed that fault may be segmented at a variety of scale, that isfrom a few meters to several tens of kilometers in length (Schwatz, 1989).

All fault segments have their boundary. The segment boundary is a portion of a fault where at least two preferable successive rupture zones have ends (Wheeler, 1989). There are several geomorphic features related to fault boundary or termination. For example, releasing bends and steps, restraining bends, branch and cross-cutting structures, and change in sense of slips, are commonly observed at segment termination of strike-slip fault (Knuepfer, 1989). For normal and reverse faults, geomorphic features defined segment endpoints is not clear (McCalpin, 1996).

Since late 1970s, many workers have found that not all faults have historical rupture records along their fault zone. Thus numbers of criteria have been conducted in order to work on fault segmentation approach such as geometric, structural, geophysical, and geological criteria. McCalpin (1996) had summarized criteria for fault segmentation into five types (Table 4.1). According to new criteria of fault segmentation have arisen, one fault has been segmented by various authors in different criteria. For example, the San Andreas Fault was divided into segments by at least four authors (Table 4.2).

In Thailand, the term "fault segmentation" was first introduced by Fenton et al. (1997) and at least two geologists show supporting evidences for fault segmentation, i.e., Won-in (1999) and Kosuwan et al. (1999). According to Fenton et al. (1997), two active faults in northern basin and range province of Thailand are recognized segmented including the Thoen Fault in Lampang and the Pua Fault in Nan. Criteria used for segmentation comprise geomorphic feature, structural style, and sense of offset. Won-in (1999) divided the Three-Pagoda fault in western Thailand into five segments based on structural, geologic, and geometric criteria. Kosuwan et al. (1999) divided the Mae Chan fault zone in Chiang Rai province into four segments based on similar criteria to those of Won-in (1999).

4.2.2 The Result of Fault Segmentation

Three criteria of fault segmentation have been used in this study, which are structural, geological, and geometric applied following those proposed by McCalpin (1996). Lineament interpretation using both Landsat TM5 and JERS imageries in the previous section plays an important role not only for locating and delineating the fault but also for segmentation the fault.

The Phrae fault system is composed of four major segments. They are the southwestern, the western, the southeastern, and the northeastern segments (Figure 4.5). The southwestern segment is located in the northern part of the Thoen basin traced along NE-trending, with the approximate length of 70 km. It has been found passing across the mountainous region between Thoen and Phrae basins. However, this fault trace becomes more complicated close to the southern part of the Phrae basin because it split into small subsegments. Moreover, the trace has not clear when get closer to that basin. The western segment has been defined bounded in the western rim of the Phrae basin in NNE-trend, and approximately 40

Table 4.1 Types of fault segments and the characteristics used to define them (after McCalpin, 1996).

Type of segment[a]	Characteristics used to define the segment[a]	Likelihood of being an earthquake segment[b]
1. Earthquake	Historic rupture limits.	By definition, 100%[c]
2. Behavioral	1) Prehistoric rupture limits defined by mutiple, well-dated paleoearthquakes.	High
	2) Segment bounded by changes in slip rates, recurence intervals, elapsed times, sense of displacement, creeping versus locked behavior, fault complexity.	Mod. (26%)
3. Structural	Segment bounded by fault branches, or intersections with other faults, folds, or cross-structures.	Mod.-High (31%)
4. Geologic	1) Bounded by Quaternary basins or volcanic fiel	Variable[d] (39%)
	2) Restriced to a single basement or rheologic terrain.	
	3) Bounded by geophysical anomalies.	
	4) Geomrphic indicators such as range-front morphology, crest elevation.	
5. Geometric	Segment defined by changes in fault orientation, stepovers, separations, or gaps in faulting.	Low -Mod. (18%)

[a]Classification follows the segment boundary types of dePolo et al. (1989,1991) and Knuepfer (1989).

[b]Percentages=percent of cases where historic ruptures have ended at this type of boundary, as opposed to rupturing through it (Knuepfer, 1989, Table 3).

[c]However, restriction of a single historic rupture to the segment does not mean that all future ruptures will be similarly restricted.

[d]Small number of observations, acculacy questionable (Knuepfer, 1989, Table 3).

Table 4.2 Fault segment lengths proposed for active faults by various authors (after McCalpin, 1996).

Fault name	Type[a]	Number of segments	Total fault length (km)	Mean segment length (km)	Modal segment length (km)	Criteria used for recognition[b]
1. Wasatch fault zone[c]	N	10	343	33	35	B,P,S,G,M
2. NE Basin and Range, >100 km[c]	N	10	-	25	20-25	B,P,S,G,M
3. NE Basin and Range, <100 km[c]	N	20	-	20	10-20	B,P,S,G,M
4. Idaho[d]	N	20	280	22	20-25	B,P,S,G,M
5. North-central Nevana[e]	N	70	-	10	10	M
6. San Adreas[f]	S	4	980	245	15-175?	B,S,G,M
6. San Adreas[g]	S	7	980	140	300?	B,P,S,M
6. San Adreas[h]	S	784	980	1.2	1	M
6. San Adreas[i]	S	68	980	14	12	M
7. San Jacinto[j]	S	20	250	12	10-15	M
8. Elsinore[k]	S	7	337	48	-	M,P
9. Xianshuihe[l]	S	1	220	220	-	M
10. Transverse Ranges[m]	R	-	-	20-30	-	M
11. Oued Fodda, Algeria[n]	R	3	32	11	11-12	B,P,S,M

[a]N,normal; S,strike-slip; R,reverse.
[b]B,behavioral; p,paleiseismic; S,structure; G,geological; M,geometric.
[c]Machette et al. (1992a).
[d]Crone and Haller (1991).
[e]Wallace (1989).
[f]Allen (1968).
[g]Wallace (1970).
[h]Wallace (1973).
[i]Bilham and King (1989).
[j]Sanders (1989).
[k]Rockwell (1989).
[l]Allen et al. (1989).
[m]Ziony and Yerkes (1985).
[n]King and Yielding (1983).

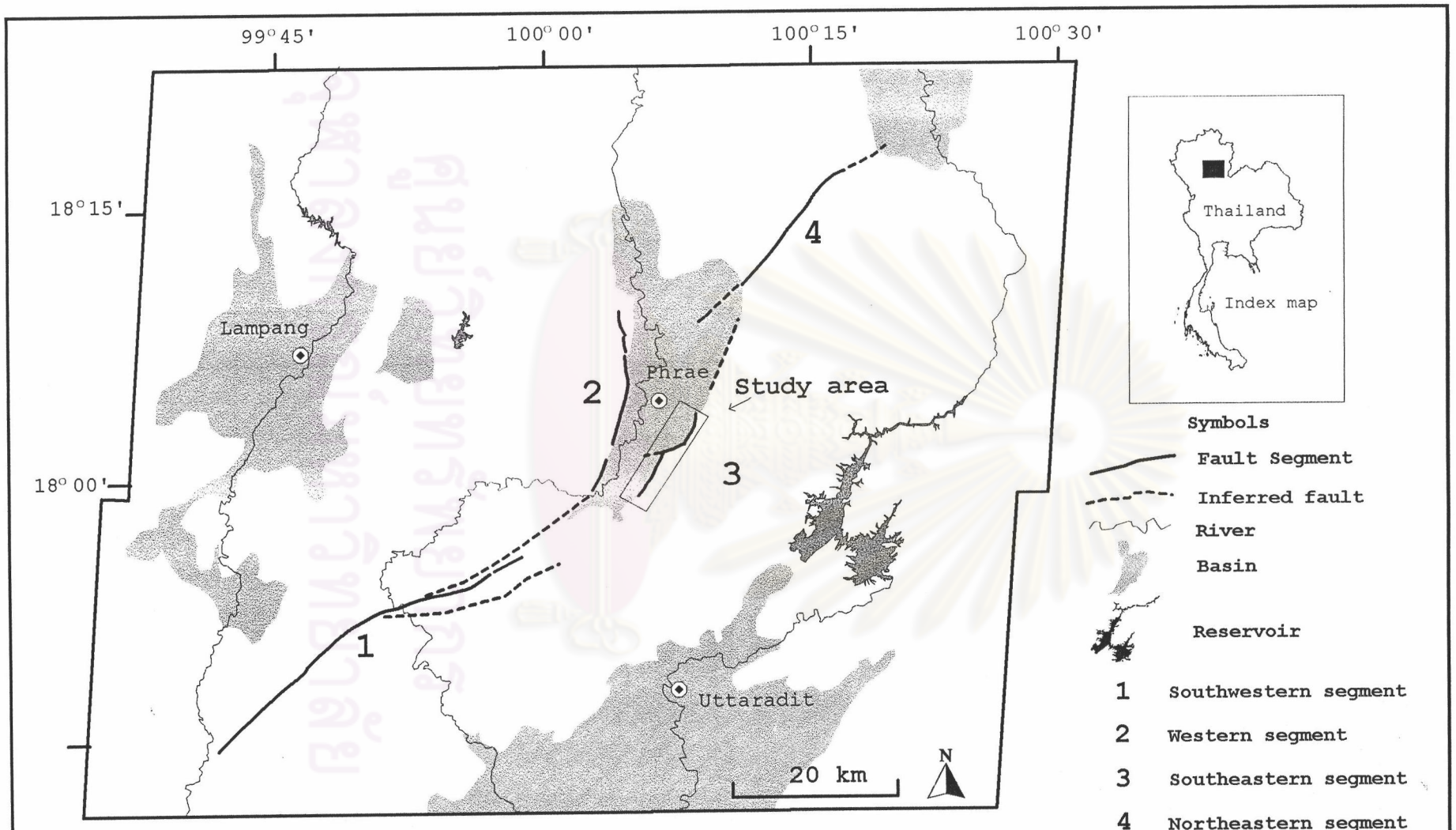

Figure 4.5 Fault segments of the Phrae fault system based on Landsat TM5 image data. The study area is shown in a box.

km-long. However, the fault trace is found bending to N-trending in the northern part with a few degrees. The southeastern segment is about 20-km-long and is NNE-trending in the southeastern portion of the Phrae basin. This fault segment is regarded as basin-bounded fault. The northeastern segment is found in the mountainous area at northeastern part outside the Phrae basin near Rong Kwang district. This segment lies in the NE-trending and seems to connect between the Phrae basin at the southwest and the Nan basin at the northeast end.

In order to study in a more detail along the southeastern segment, further segmentation has been conducted, based on structural, geological, and geometric information, and lineament data from both Landsat TM and JERS images. The southeastern segment can be divided into three subsegments (Figure 4.6), namely, Ban Thung Charoen subsegment, located in the south of the study area, Ban Kwang subsegment located in the central, and Ban Pa Daeng subsegment located in the north. According to the lineament interpretation data in previous section, it is concluded that they are corresponding to three major lineaments previously mentioned (see section 4.1). By comparison, Ban Thung Chareon subsegment is referred to the southern NNE-trending, Ban Kwang subsegment to the central ENE-trending, and Ban Pa Daeng subsegment resembling the northern NNE-trending lineaments.

Although these three subsegments can be delineated using both satellite images (Figure 4.7), these subsegments cannot be traced continuously by using aerial photographs. However, several fault branches are observed (Figure 4.8). The major trend of fault branches lies in the NNE direction and the minor ones in the NW and ENE directions. These fault branches are short with the shortest one about 0.25 km and the longest about 2.0 km. There are nine fault branches lying along Ban Thung Charoen subsegment. One of these fault branches can be traced to Ban Kwang subsegment. Along Ban Pa Deang subsegment, eleven fault branches have been observed.

Besides, according to structure associated with an idealized strike-slip fault model constructed by Christie-Blick and Biddle (1985), these fault branches should be the component of shear zone, which are synthetic, secondary synthetic, and antithetic shears (Figure 4.9). All of these shear zone features are accommodated in principal displacement zone (PDZ).

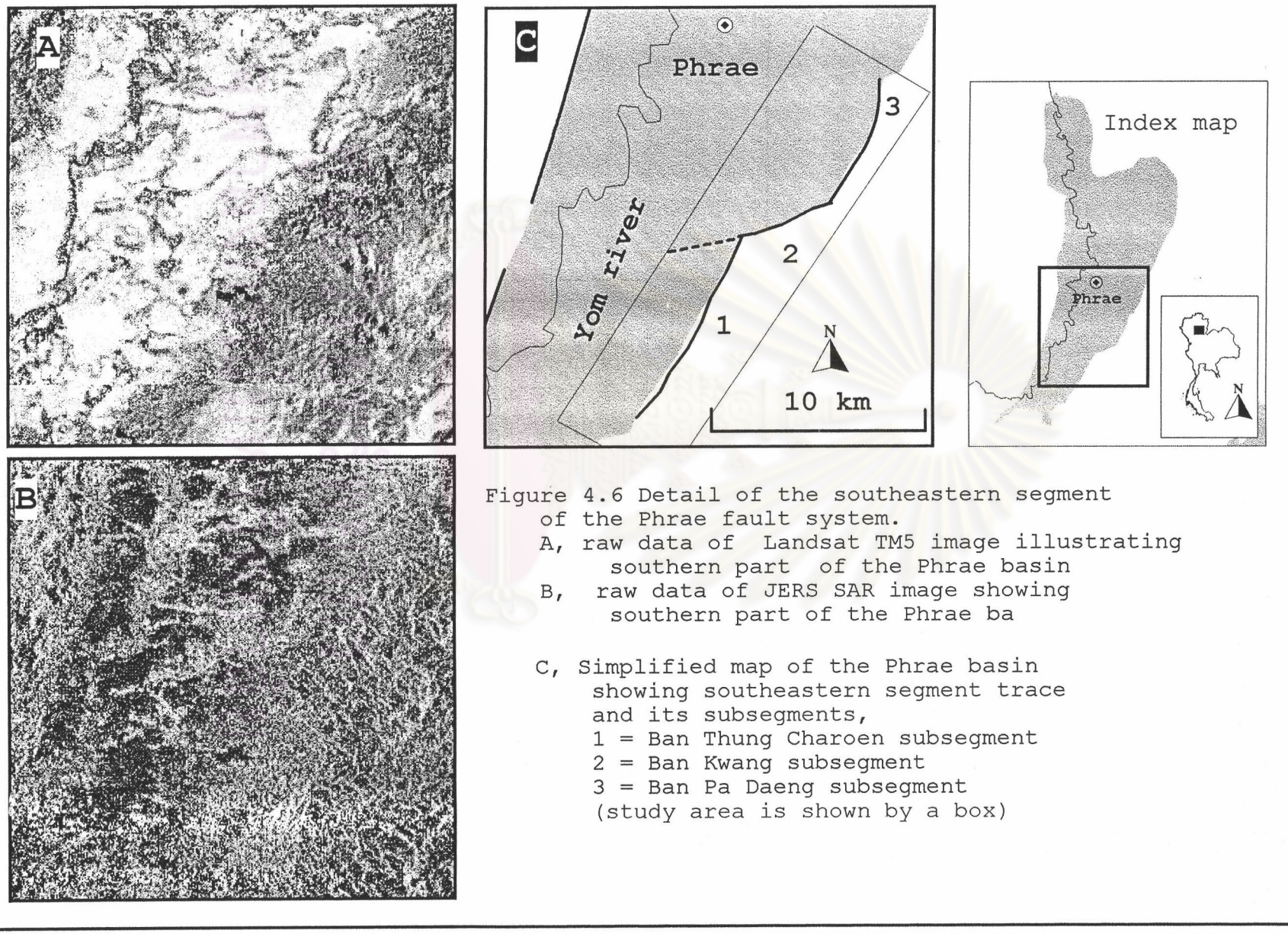

Figure 4.6 Detail of the southeastern segment of the Phrae fault system.
A, raw data of Landsat TM5 image illustrating southern part of the Phrae basin
B, raw data of JERS SAR image showing southern part of the Phrae ba

C, Simplified map of the Phrae basin showing southeastern segment trace and its subsegments,
1 = Ban Thung Charoen subsegment
2 = Ban Kwang subsegment
3 = Ban Pa Daeng subsegment
(study area is shown by a box)

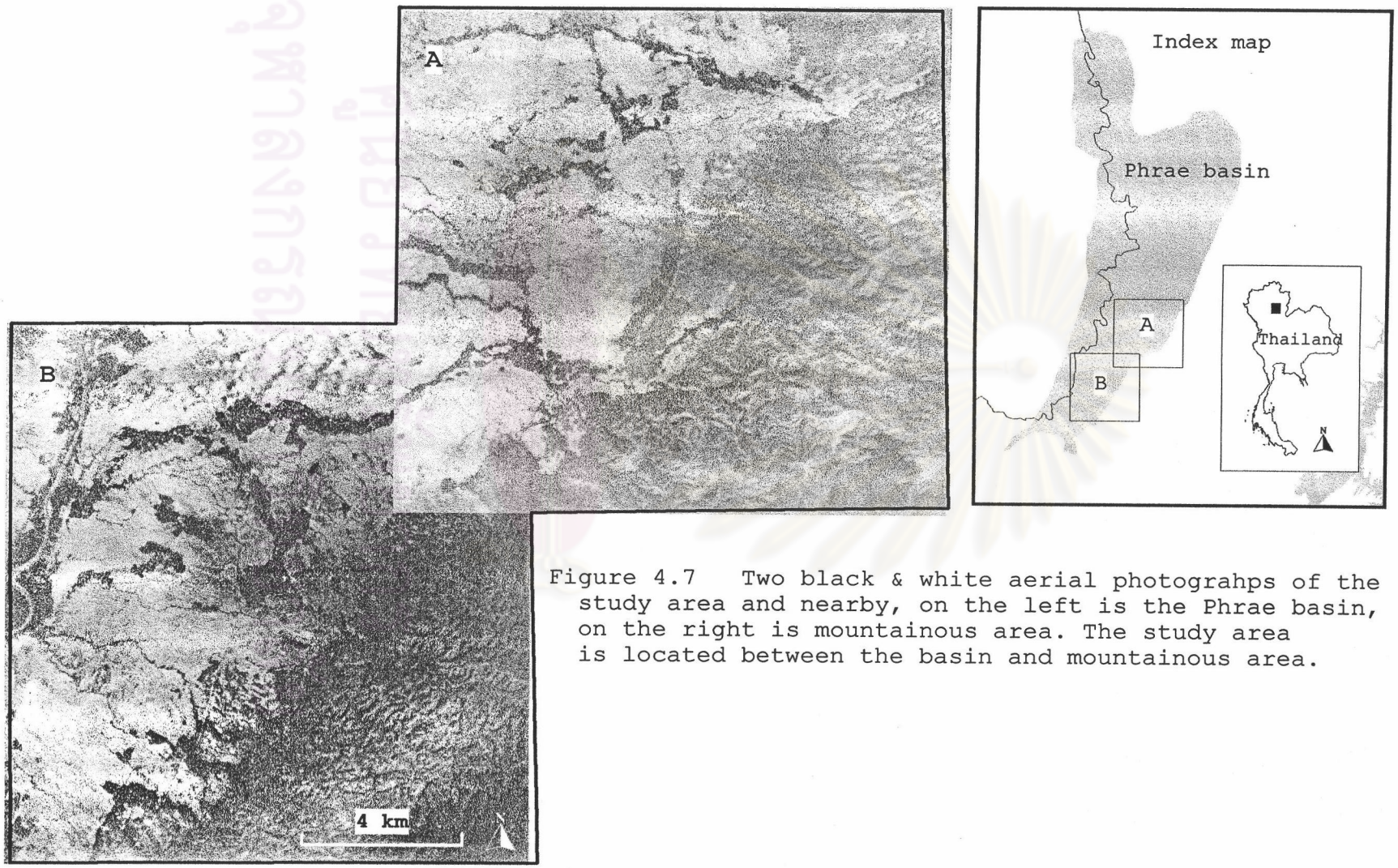

Figure 4.7 Two black & white aerial photograhps of the study area and nearby, on the left is the Phrae basin, on the right is mountainous area. The study area is located between the basin and mountainous area.

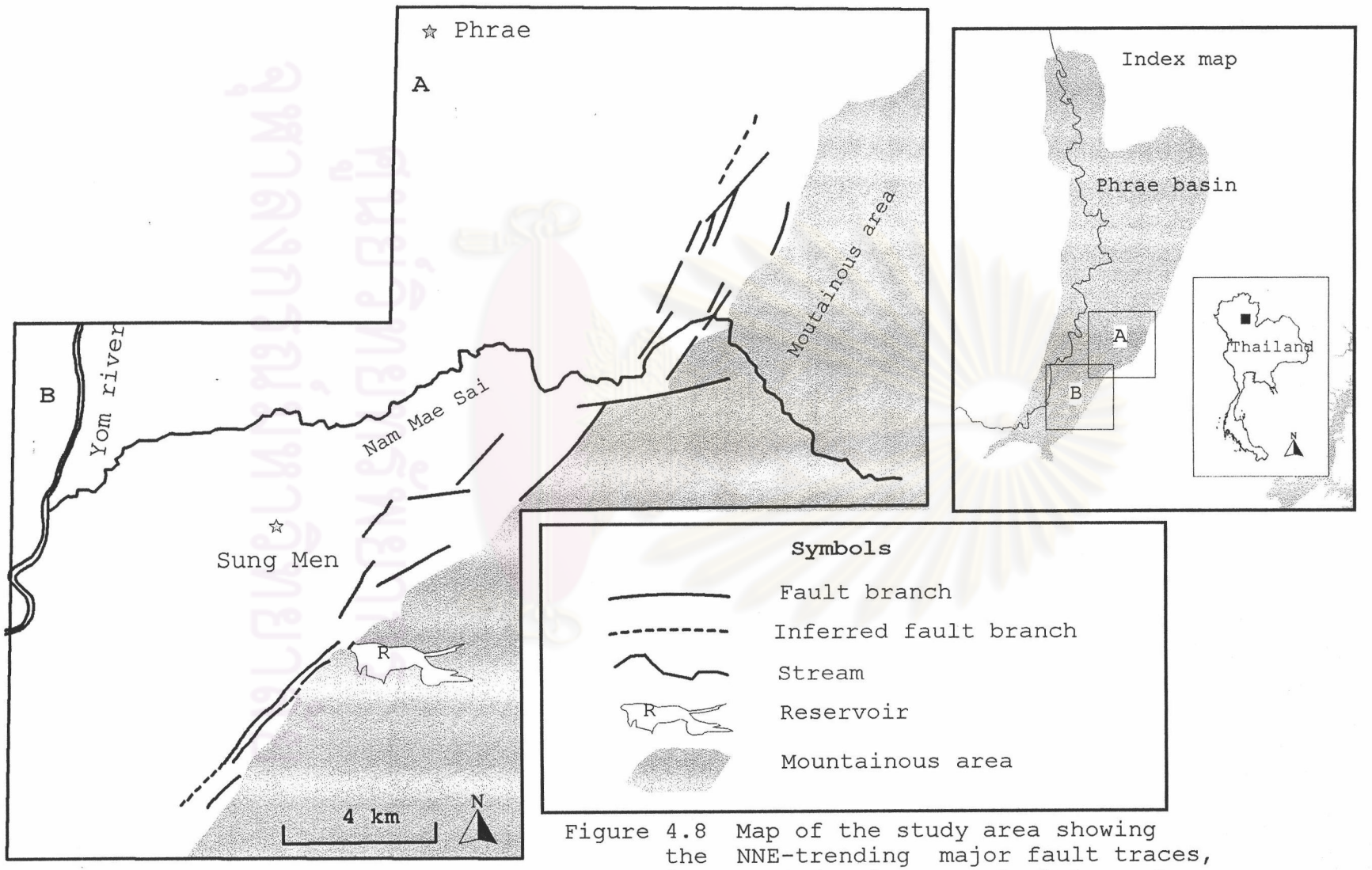

Figure 4.8 Map of the study area showing the NNE-trending major fault traces, interpreted using aerial photograph.

4.3 Tectonic Geomorphology

4.3.1 General

In this section, basic concepts of tectonic geomorphology of which related to three types of faults, namely, strike-slip, normal, and reverse, are briefly explained. The discussion will be followed by methodology and the result of this thesis study.

According to strike-slip fault zone, a variety of structure and landforms can be originated by simple shear including fractures, folds, normal faults, trust faults, and reverse faults (Figure 4.10)(Keller & Pinter, 1996). Naturally, within a broad shear zone, different generation of motion have produced various kinds of these structure which all of them can be superimposed and showing array of structural complexity (Sylvester, 1988). In many strike-slip faults, bending fault trace can be observed at overlapping areas between the adjacent blocks. Therefore fault movement can create both compressive and tensile stresses into the curve of fault segments. For instance, as shown in Figure 4.11, releasing bend and restraining bend can cause pull-apart basins and uplift features related to tension and compression stresses, respectively (Biddle and Christie-Brick, 1985). In many cases, both pull-apart basins and uplift highs may be explained in term of step-over in which two fault segments have end up, and both showing the same sense of movements.

In conclusion, there are many features of tectonic geomorphology produced by strike slip movement. As shown in Figure 4.12 these features are linear valleys, offset or deflected streams, shutter ridges, sag pones, pressure ridges, benches, scarps and small horsts and garbens (Keller, 1986). Noteworthy, fluvial terraces, stream channels, and alluvial fans are typical features used to reconstruct paleoearthquake offset history (Weldon II et al., 1996).

Besides, based on simple shear model illustrating in Figure 4.10, normal fault trace should be formed perpendicular to the direction of maximum elongation and maximum extension stress. Figure 4.13 shows an idealized cross-section of extension tectonic environments. Master fault has bounded the main on the right, accompanied by minor synthetic and antithetic faults. Other structures commonly found in an extension regime are horsts and grabens showing on the left. Depending on tectonic geomorphology on ground surface, typical indicator of

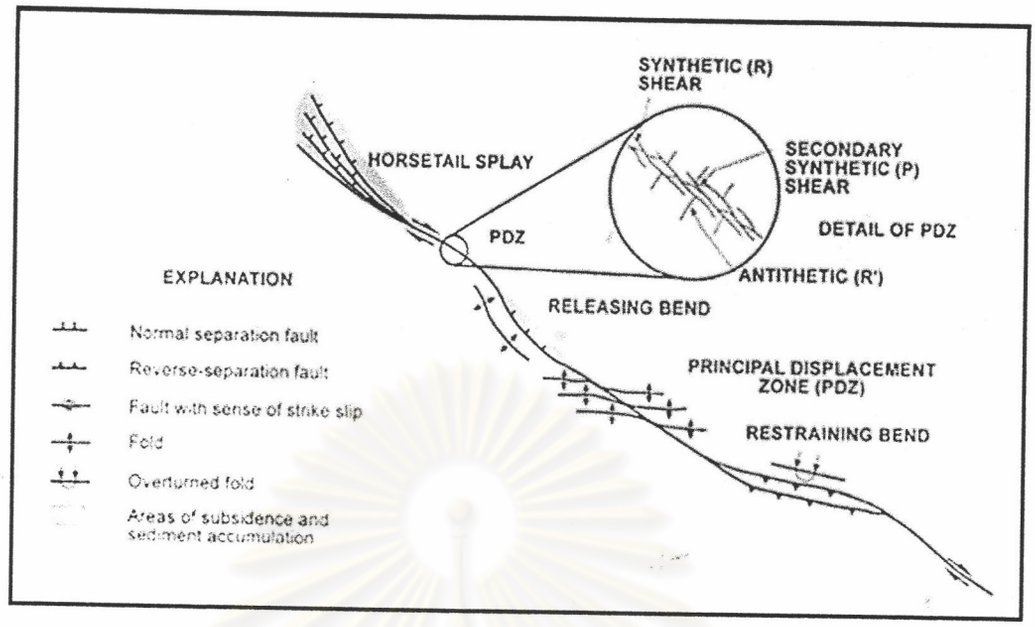

Figure 4.9 Plan view of structure associated with an idealized strike-slip fault (after Christie-Blick & Biddle, 1985).

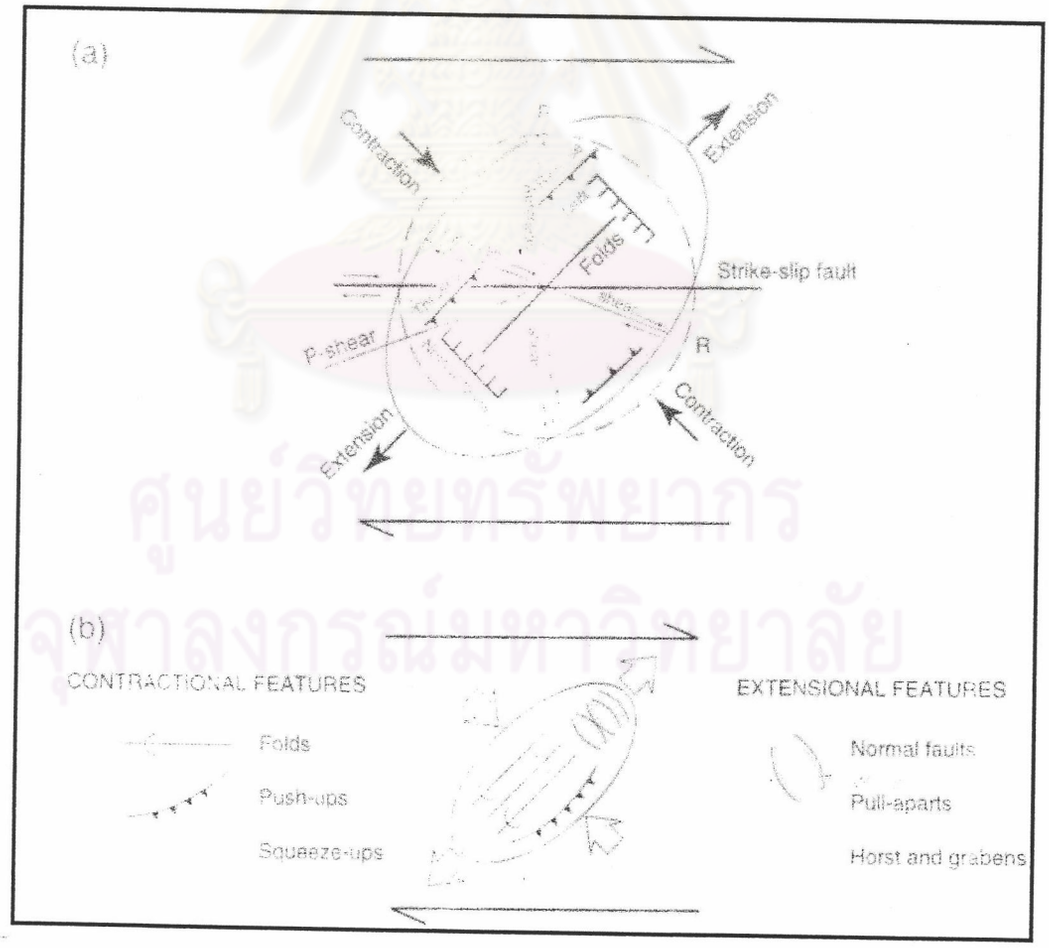

Figure 4.10 Simple shear model associated with strike-slip fault (a), producing contractional and extensional features (b) (after Keller & Pinter, 1996).

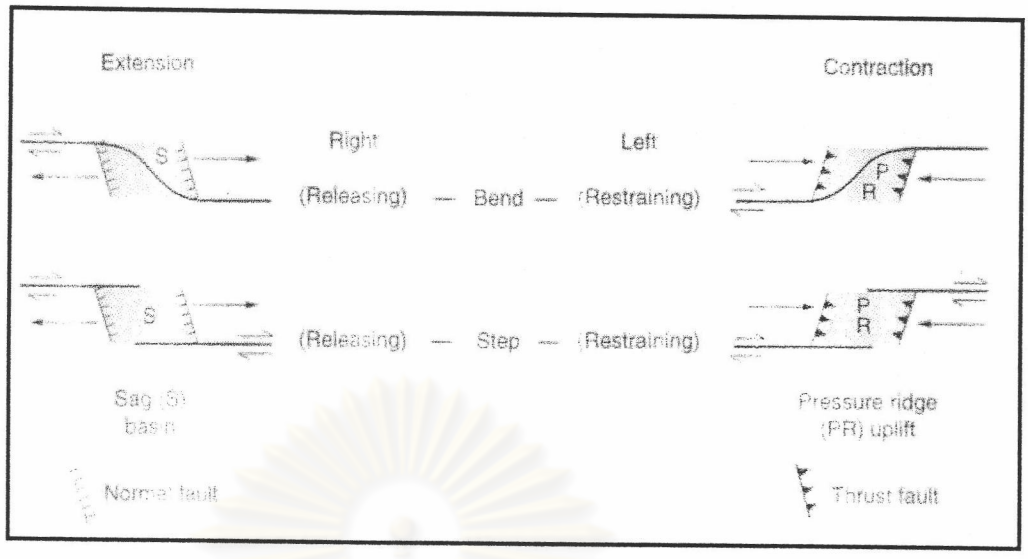

Figure 4.11 Sag and pressure ridges associated with bend and steps along strike-slip faults (after Keller & Pinter, 1996).

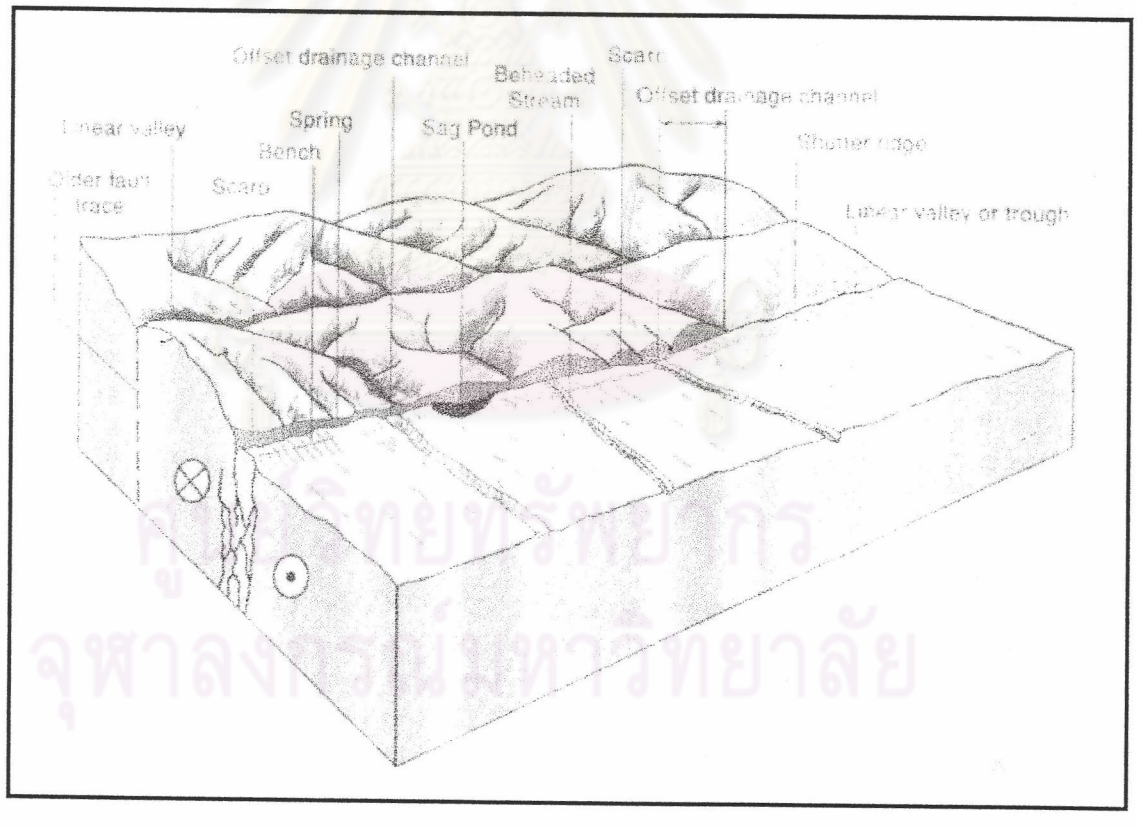

Figure 4.12 Assemblage of landform associated with active tectonic strike-slip faulting (after Burbank & Anderson, 2001).

normal faulting is a fault scarp (Figure 4.14), which can be developed to form triangular facets when proper condition such as erosion and repetition of active fault movement has reached (Figure 4.15). In addition, other evidences of extension environments consist of linear-range fronts, escarpments, volcanic (lava flows, cones, etc), rift valleys and axial rifts of oceanic ridge systems (Keller & Pinter, 1996).

Lastly, tectonic landforms associated to reverse faulting include belt of active folding and faulting, steep mountain fronts, and fault scarps. The elongated axis of these structures is usually found lied perpendicular to the direction of maximum compressive stress axis as show in figure 4.11. The most common geomorphic evidence of compression tectonism in continent is fault scarp (Carver & McCalpin, 1996). Based on historical surface ruptures in Armenia (1988) earthquakes, seven types of trust fault scarp morphology have been conducted by Phillip et al.(1992)(Figure 4.16).

In Thailand, Fenton et al.(1997) had revealed several tectonic geomorphology found along seven faults in northern basin and range province of Thailand. These morphologies include linear-range fronts, triangular facets, offset drainages, stream knick points, wine-glass canyons, and scarps. Won-in (1999) mentioned that fault scarps, triangular facets, offset stream channels, shutter ridges, beheaded streams, pressure ridges, fault trace cutting terraces, basin development, parallel ridges, and uplift river gravel deposit are observed along the Three-Pagoda fault zone. Kosuwan et al. (1999) stated that several tectonic geomorphology such as offset streams, sag ponds, shutter ridges, and benches (river terraces)on young alluviums/colluviums, have been observed along the Mae Chan fault zone.

4.3.2 Results of Tectonic Geomorphological Study

According to this study, tectonic geomorphological results are mainly conducted using aerial photographic interpretation. Tectonic geomorphological map was compiled in order to characterize general tectonic features (Figure 4.17). Three types of evidences related to fault movement have been found. There are clearly defined offset stream channels, triangular facets, and a shutter ridge (Figure 4.18). Firstly, two offset stream channels were observed in the southernmost part of the Ban Thung Charoen subsegment close to a mountain front.

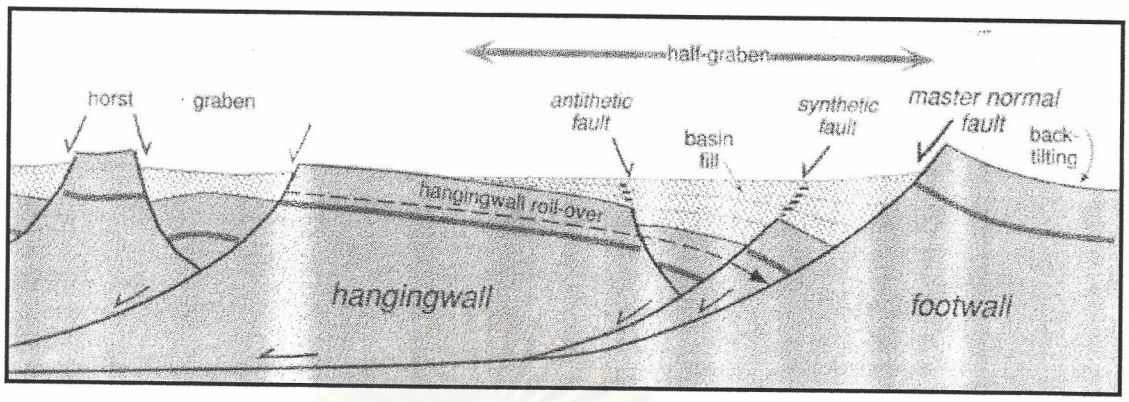

Figure 4.13 Idealized cross-section of extension tectonic environments (after Burbank & Anderson, 2001).

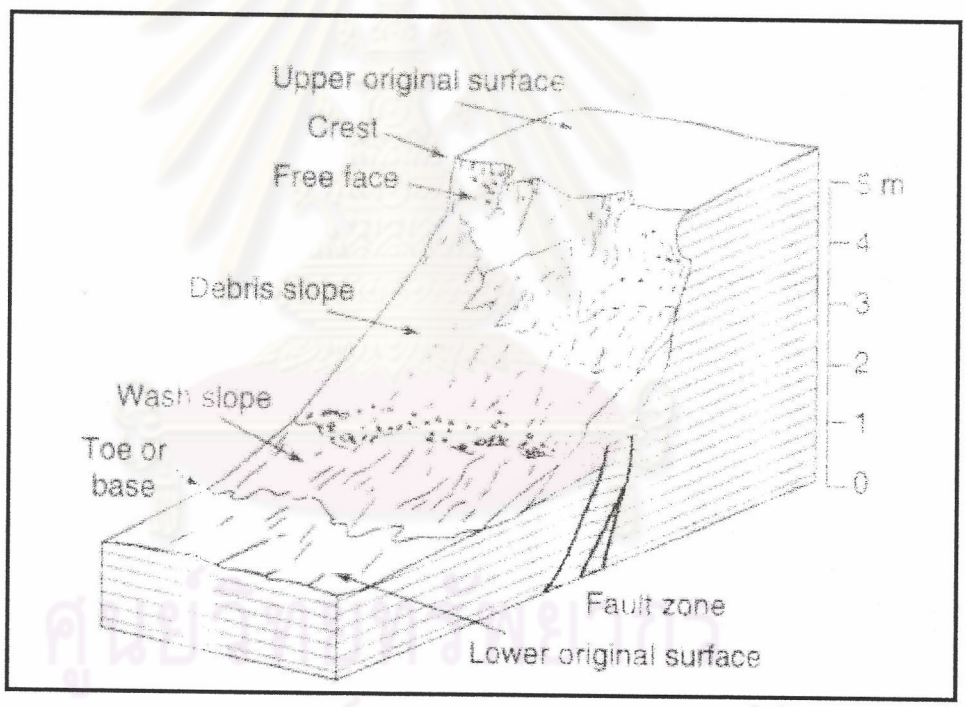

Figure 4.14 Basic slope elements that may be present on a fault scarp (after McCalpin, 1996).

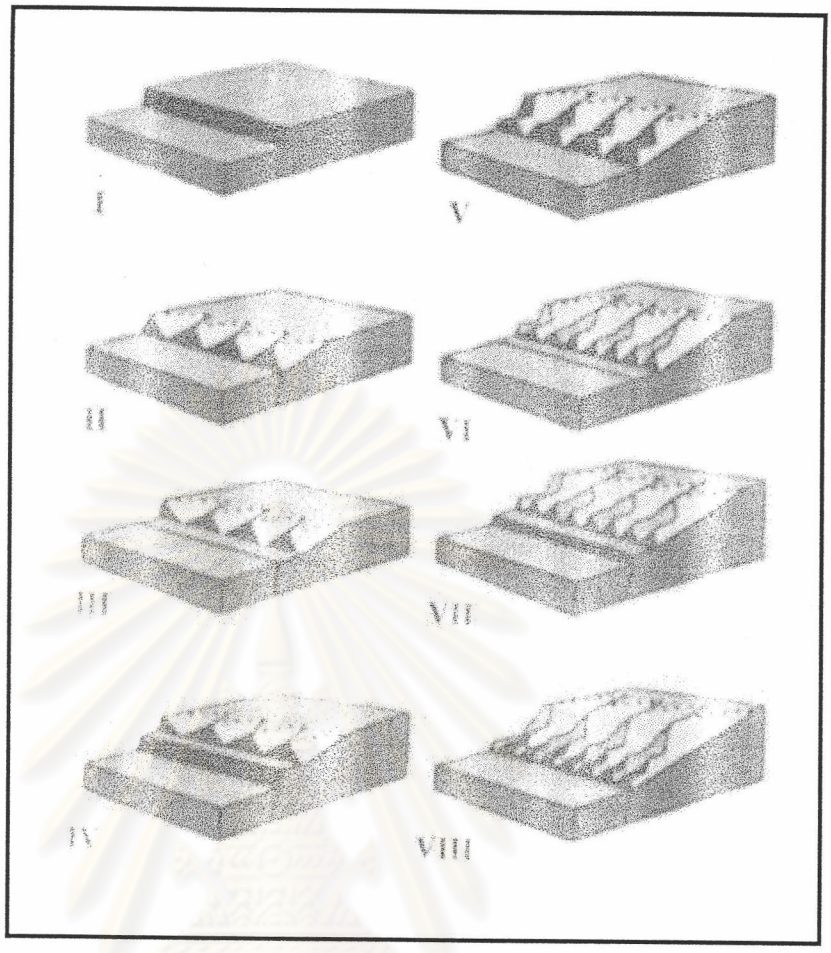

Figure 4.15 Development of triangular facets produced by episodic vertical tectonic movement. I: Undissected fault scarp. II: development of faceted spurs by stream cutting across the fault scarp. III: period of tectonic quiescence with slope retreat, and development of narrow pediment. IV: renewed fault movement. V: dissection of the new fault scarp by major streams and streams developed on the faces of the facet spurs developed at stage II. VI: a new period of tectonic quiescent, with the development of another narrow pediment within the footwall block at the base of the range front. VII: renewed fault movement. VIII: dissection of the fault scarp produced at stage VII resulting in the line of small facet spurs at the base of the range front. Remnants of narrow pediments (benches) are preserved at the apices of each set of faceted spurs. Progressive slope retreat is accompanied by a decrease in the slope angle of the faceted spurs (after Fenton et al., 1997).

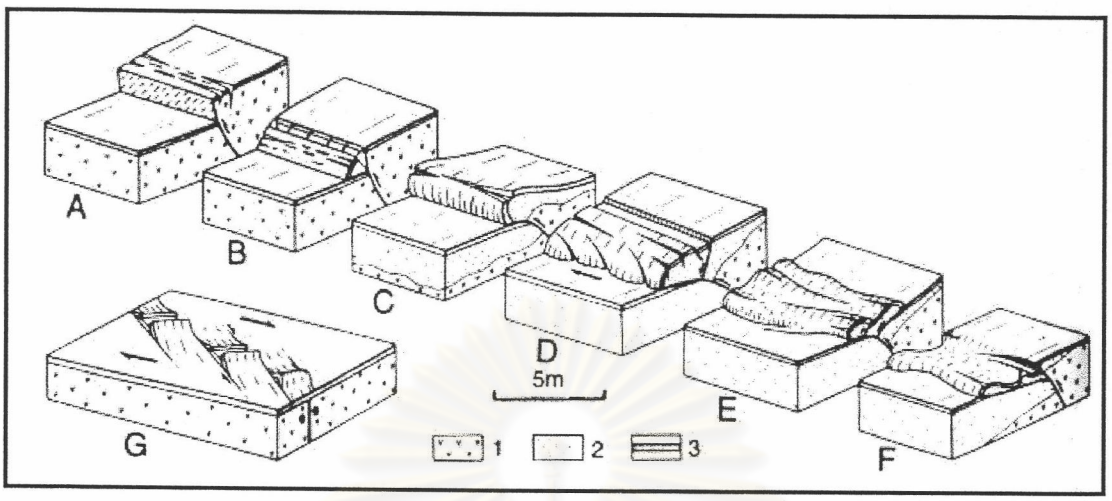

Figure 4.16 Types of reverse fault scarps. (A) Simple reverse (or trust) scarp. (B) Hangingwall collapse scarp. (C) Simple pressure ridge. (D) Dextral pressure ridge. (E) Back-trust pressure ridge. (F) Low-angle ridge. (G) En-echelon pressure ridge. 1,bed rock; 2, soft Quaternary sediments; 3, turf (after McCalpin, 1996).

Generally, in this area the streams flow from the mountainous area in the east to the basin in the west (Figure 4.19). However, in some location the stream changed their flow direction due to faulting. These offset streams indicate a left-lateral movement with an average of offset length of about 0.5 km along the fault. Secondly, two sets of triangular facets have been observed in the central part of the study area. The first set with an average base of 1.5 km and average height of 40 m, is located in the northern end of Ban Thung Chareon subsegment, and is composed of two west-dipping facets developed on the NNE-trending fault branch. The second set with the average base of 0.7 km and the average height of 40 m, is observed along the ENE-trending Ban Kwang subsegment, displaying four facet spurs. The prominent triangular facets support the evidence that these fault subsegments had once experienced with normal movement. A shutter ridge, which is about 0.5 km-long and 25 m-high, is found lying along Ban Kwang subsegment in front of the second set of triangular facets. This ridge blocks a stream channel that flows straight forwards from mountainous area. Subsequently, the stream has changed its flow direction to sinistral. According to this tectonic evidence, Ban Kwang subsegment should be displaced with left-lateral movement in the past.

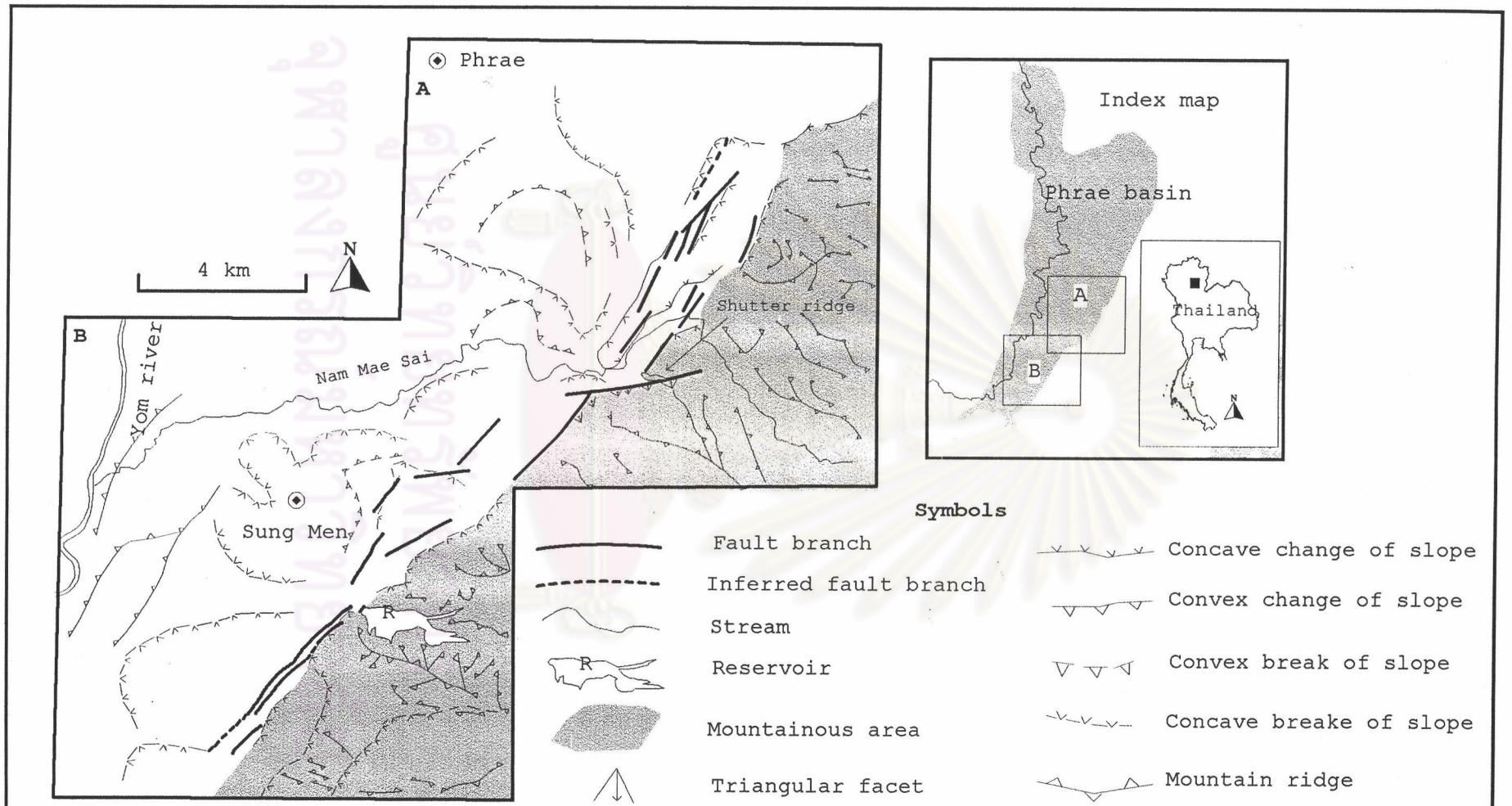

Figure 4.17 Tectonic geomorphological map along the southeastern segment of the Phrae fault system.

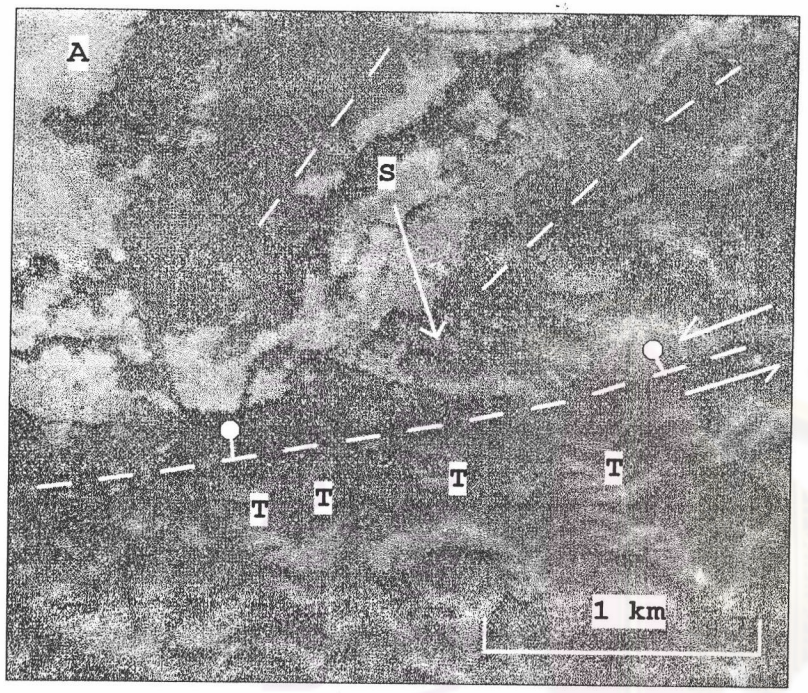

Figure 4.18 Tectonic geomorphological evidence observed from aerial photograph.

A, Magnified aerial photo showing the location of triangular facets (T) and a shutter ridge(S), these evidences indicated normal-sinistral movement.

B, Magnified aerial photograph showing the location of offset strem channels which indicated sinistral movement.

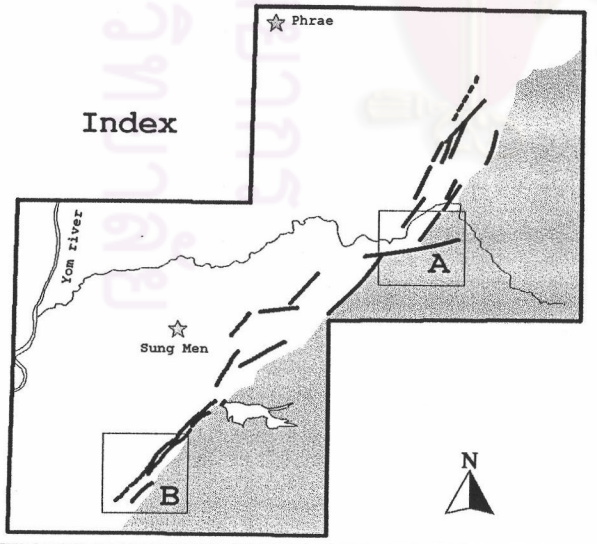

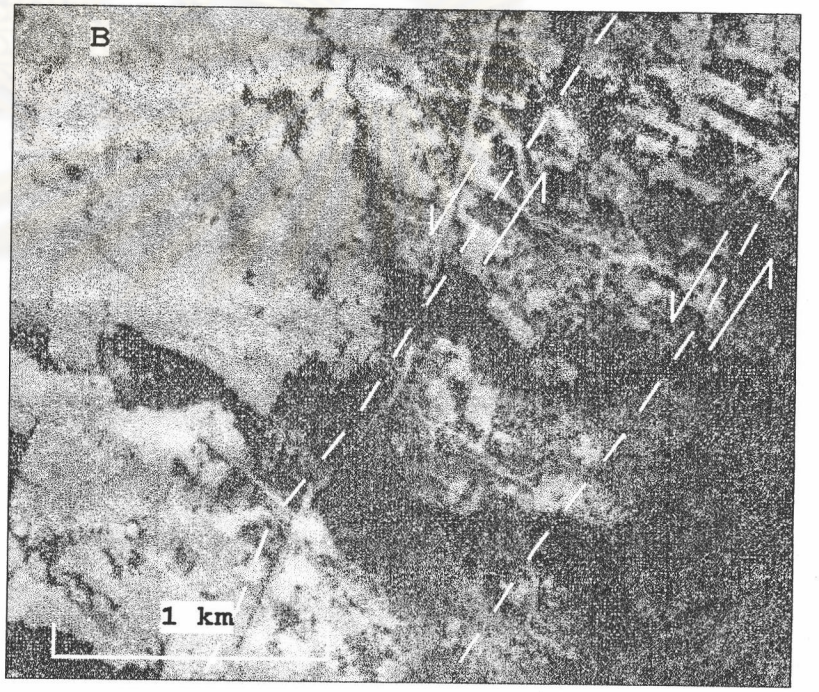

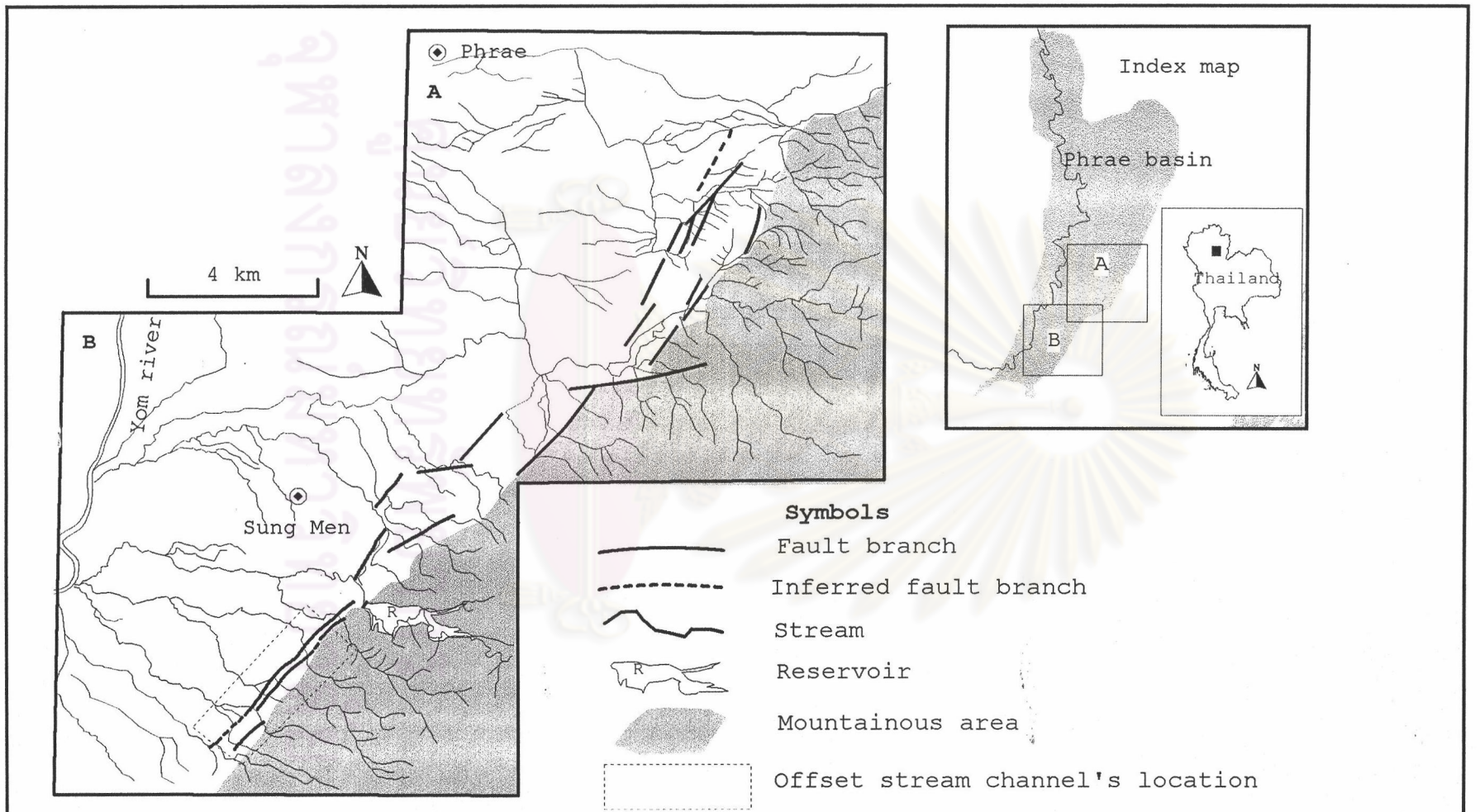

Figure 4.19 Drainage pattern of the study area and nearby based on aerial photographic interpretation, flow direction is from mountainous area in the east to basin in the west. Offset streams by sinistal movement is in box.

In summary, based on aerial photograph interpretation, tectonic geomorphological evidence found in Ban Thung Charoen and Ban Kwang subsegments, should be indicated as normal-sinistral displacement. Besides, in Ban Pa Daeng subsegment, there was no evidence of tectonic geomorphology observed using aerial photograph.